Post-Infarction Risk Prediction with Mesh Classification Networks

Marcel Beetz[1(✉)], Jorge Corral Acero[1], Abhirup Banerjee[1,2], Ingo Eitel[3,4,5], Ernesto Zacur[1], Torben Lange[6,7], Thomas Stiermaier[3,4,5], Ruben Evertz[6,7], Sören J. Backhaus[6,7], Holger Thiele[8,9], Alfonso Bueno-Orovio[10], Pablo Lamata[11], Andreas Schuster[6,7], and Vicente Grau[1]

[1] Institute of Biomedical Engineering, Department of Engineering Science, University of Oxford, Oxford, UK
marcel.beetz@eng.ox.ac.uk
[2] Division of Cardiovascular Medicine, Radcliffe Department of Medicine, University of Oxford, Oxford, UK
[3] University Heart Center Lübeck, Medical Clinic II, Cardiology, Angiology, and Intensive Care Medicine, Lübeck, Germany
[4] University Hospital Schleswig-Holstein, Lübeck, Germany
[5] German Centre for Cardiovascular Research, Partner Site Lübeck, Lübeck, Germany
[6] University Medical Center Göttingen, Department of Cardiology and Pneumology, Georg-August University, Göttingen, Germany
[7] German Centre for Cardiovascular Research, Partner Site Göttingen, Göttingen, Germany
[8] Department of Internal Medicine/Cardiology, Heart Center Leipzig at University of Leipzig, Leipzig, Germany
[9] Leipzig Heart Institute, Leipzig, Germany
[10] Department of Computer Science, University of Oxford, Oxford, UK
[11] Department of Biomedical Engineering, King's College London, London, UK

Abstract. Post-myocardial infarction (MI) patients are at risk of major adverse cardiac events (MACE), with risk stratification primarily based on global image-based biomarkers, such as ejection fraction, in current clinical practice. However, these metrics neglect more subtle and localized shape differences in 3D cardiac anatomy and function, which limit predictive accuracy. In this work, we propose a novel geometric deep learning approach to directly predict MACE outcomes within 1 year after the infarction event from high-resolution 3D cardiac anatomy meshes. Its architecture is specifically designed for direct and efficient processing of surface mesh data with a hierarchical, multi-scale structure to enable both local and global feature learning. We evaluate the binary MACE prediction capabilities of the proposed mesh classification network on a multi-center dataset of post-MI patients. Our results show that the proposed method outperforms corresponding clinical benchmarks by ∼16% and ∼6% in terms of area under the receiver operating characteristic (AUROC) curve for 3D shape and 3D contraction inputs, respectively. Furthermore, we visually analyze both 3D cardiac shapes and 3D contraction patterns with regards to their MACE predictability and demonstrate how task-specific information learned by the network on a balanced

O. Camara et al. (Eds.): STACOM 2022, LNCS 13593, pp. 291–301, 2022.
https://doi.org/10.1007/978-3-031-23443-9_27

dataset successfully generalizes to increasing levels of class imbalance. Finally, we compare our approach to both clinical and machine learning benchmarks on our original highly-imbalanced dataset of post-MI patients and find average improvements in AUROC scores of ∼9% and ∼3%, respectively.

Keywords: Major adverse cardiac event prediction · 3D cardiac shape · 3D cardiac contraction · Graph neural networks · Mesh pooling · Post-myocardial infarction · Cardiac MRI · Geometric deep learning

1 Introduction

Ischemic heart disease is the most common cause of death worldwide with cases continuing to increase [18]. While progress has recently been made in predicting myocardial infarction (MI) outcomes, post-MI patients are still at risk of recurrent major adverse cardiac events (MACE) [15,18,23,25]. In order to correctly stratify post-MI patients into risk groups and determine suitable preventative measures, cardiac magnetic resonance imaging (MRI) is considered as the gold standard imaging modality as it enables the accurate calculation of widely used image-based biomarkers, such as ejection fraction, and the characterization of left ventricular (LV) anatomy and function [8,15,23,28]. However, such biomarkers only provide a global assessment in the form of a single value, thus neglecting more localized patterns in the complex 3D cardiac physiology, which have been shown to play an important role in the management of post-MI patients [9]. Accordingly, previous works have focused on discovering novel predictive biomarkers by analyzing more subtle aspects of the 3D cardiac shapes [9,14,29].

In the recent past, deep learning has revolutionized the field of medical image analysis and outperformed previous approaches in a variety of different tasks, including clinical outcome prediction [6]. Specifically for anatomical surface data, geometric deep learning methods have been shown to be highly suitable for creating more detailed models of cardiac anatomy and function, using both graph [12,21,22,24] and point cloud-based [1–5,7] processing. Building on these developments, we present in this work a novel mesh classification network to predict MACE outcomes based on 3D shape information of cardiac anatomy and function. Its architecture utilizes recent advances in geometric deep learning to enable direct and targeted processing of high-resolution mesh data and efficient feature learning at both local and global scales to facilitate the usage of more advanced image-based biomarkers. To the best of our knowledge, this is the first deep learning approach for direct 3D shape-based MACE prediction in post-MI patients.

2 Methods

2.1 Overview

We present an overview of our proposed approach for the prediction of MACE outcomes with mesh classification networks in Fig. 1.

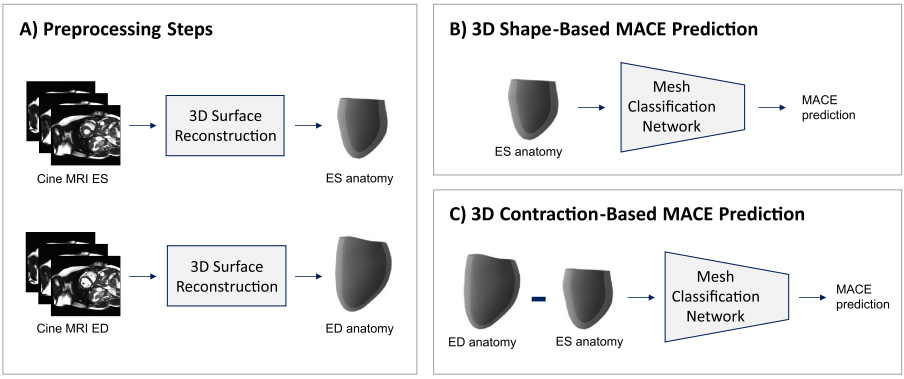

Fig. 1. Overview of the proposed mesh-based deep learning approach for prediction of major adverse cardiac events (MACE). First, 3D surface meshes of the cardiac anatomy at ED and ES are reconstructed from cine MRI acquisitions in a preprocessing step (A). Next, 3D cardiac anatomies at ES are input into a mesh classification network for 3D shape-based MACE prediction (B). Finally, the vertex-wise differences between anatomy meshes at ED and ES are used as representations of 3D contractions to predict MACE outcomes with a separate mesh classification network (C).

We first select cardiac magnetic resonance (MR) images at both the end-diastolic (ED) and end-systolic (ES) phases of the cardiac cycle as our input data. In order to obtain high-resolution 3D representations of cardiac shapes, we apply a fully automatic multi-step surface reconstruction pipeline as a preprocessing step (Fig. 1-A) (Sect. 2.2). We then use the reconstructed meshes at ES and the vertex-wise differences between ED and ES meshes to train and evaluate separate mesh classification networks for 3D shape-based (Fig. 1-B) and 3D contraction-based (Fig. 1-C) binary MACE prediction, respectively (Sect. 2.3).

2.2 Dataset and Preprocessing

The dataset used in this work consists of cine MR images of 1021 post-MI patients acquired as part of two multi-center trials, TATORT-NSTEMI (Thrombus Aspiration in Thrombus Containing Culprit Lesions in Non-ST-Elevation Myocardial Infarction; NCT01612312) [30] and AIDA-STEMI (Abciximab Intracoronary Versus Intravenously Drug Application in ST-Elevation Myocardial Infarction; NCT00712101) [16]. Major adverse cardiac events (either reinfarction,

new congestive heart failure, all-cause death, or any combination of these) 12 months post-MI was chosen as the study endpoint, and 74 patients were recorded with this outcome. In order to obtain the 3D LV anatomy meshes required for our proposed 3D shape-based MACE classification networks, we first pass the MR images of the dataset through a multi-step surface reconstruction pipeline [9]. The pipeline consists of both a segmentation step, which uses deep convolutional neural networks with customized data augmentation to extract the LV contours from the raw short-axis MRI slices [10,11], and a mesh fitting step which positions and deforms a 3D LV template mesh to fit the extracted contours [20]. A detailed description of the pipeline can be found in [9].

2.3 Network Architecture and Training

The architecture of our proposed mesh classification network combines recent advances in graph convolutions and mesh sampling with multilayer perceptrons in a hierarchical cascade structure (Fig. 2).

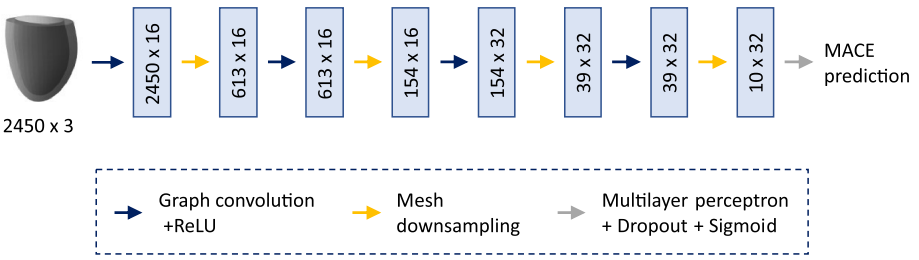

Fig. 2. Architecture of the proposed mesh classification network. High-resolution input meshes are processed by a cascade of graph convolution and mesh downsampling layers followed by a multi-layer perceptron with dropout and a sigmoid activation function to enable efficient multi-scale feature learning for binary MACE prediction.

The network inputs are 3D triangular meshes with 2450 vertices and shared vertex connectivity across the dataset. The meshes either represent the LV surfaces at ES or the per-vertex deformation between ED and ES. The inputs are passed through four levels of spectral graph convolution and mesh downsampling layers to enable efficient multi-scale feature learning directly on mesh data. A multi-layer perceptron followed by a sigmoid function is then applied to obtain the predicted output probabilities for the binary MACE classification task. We compute all graph convolutions with the Chebyshev polynomial approximation [13] of order 5 and subsequently apply rectified linear units (ReLU) as activation functions. All mesh pooling layers are implemented using quadric error minimization [27]. Furthermore, we include drop-out layers after each fully connected layer as a regularizer to improve generalizability. We train on a CPU using the Adam optimizer [19] with a batch size of 32 and a binary cross entropy loss function,

until loss convergence is achieved on the validation dataset. The mesh classification networks are implemented using the PyTorch [26] and Pytorch Geometric [17] frameworks.

3 Experiments and Results

3.1 End-Systolic Shape-Based Prediction

We first aim to assess the ability of the mesh classification network to predict binary MACE outcomes based solely on 3D cardiac surface meshes at ES. As a clinical benchmark, we choose ES volume to encapsulate cardiac shape at ES and input the values as the independent variable into a logistic regression model with binary MACE outcomes as the dependent variable. To facilitate effective feature learning for both approaches, we select a dataset with a balanced representation of MACE and Non-MACE cases by randomly sampling a subset of Non-MACE cases (n = 74) from the original dataset and apply 3-fold cross validation in our experiment. We report in Table 1 the averaged results across the respective unseen test folds in terms of widely used binary classification metrics.

Table 1. ES Shape-based MACE prediction results on balanced dataset.

Input	AUROC	Accuracy	Precision	Recall	F1-score
ES volume	0.624	0.605	0.604	0.633	0.614
ES 3D shape	0.721	0.721	0.718	0.710	0.717

We find that the mesh classification network achieves considerably higher scores than the clinical benchmark across all metrics, including a ∼15.5% performance improvement in cross-validated area under the receiver operating characteristic (AUROC) curve.

Next, we want to investigate which types of 3D meshes cause the network to give accurate predictions. To this end, we calculate the absolute differences between the network's predicted output probabilities and the respective ground truth encodings of either MACE or Non-MACE. Hereby, a small difference value indicates a very good prediction by the network for both outcome possibilities and vice versa for large difference values. Based on these prediction error values, we select and visualize in Fig. 3 three sample cases corresponding to the network's good prediction of MACE, good prediction of Non-MACE, bad prediction of MACE, and bad prediction of Non-MACE.

We observe that the network typically predicts MACE outcomes for hearts with larger volumes and smaller myocardial thickness. Bad network predictions are more likely to occur if this association is less clear or reversed for the particular case, e.g. a smaller LV volume with a MACE outcome.

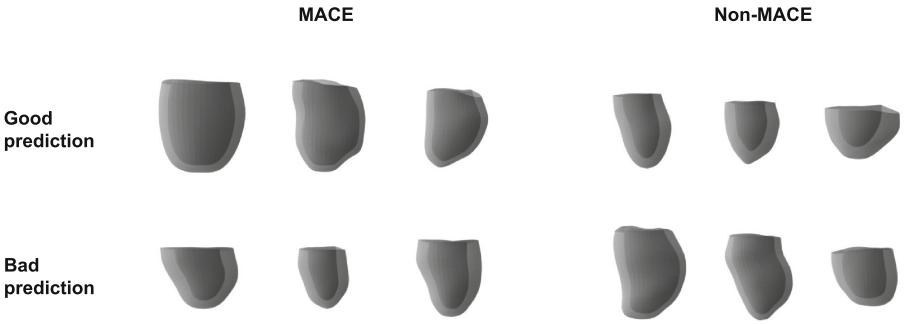

Fig. 3. Input ES meshes that resulted in good (row 1) and bad (row 2) predictions for ground truth MACE (column 1) and Non-MACE (column 2) cases respectively by the shape-based mesh classification network.

3.2 Contraction-Based Prediction

In addition to ES 3D shape, we also want to study the utility of 3D contractions for MACE prediction. We therefore repeat the same experiment of the last section but pass meshes that represent vertex-wise differences between ED and ES shapes as inputs to a separate mesh classification network. Since this gives the network access to both ED and ES shapes, we also choose a different clinical metric, ejection fraction, as the independent variable in our logistic regression. The averaged results of the respective 3-fold cross validation experiments are depicted for both methods in Table 2.

Table 2. Contraction-based MACE prediction results on balanced dataset.

Input	AUROC	Accuracy	Precision	Recall	F1-score
Ejection fraction	0.696	0.666	0.705	0.581	0.633
3D contraction	0.738	0.726	0.732	0.712	0.719

We find that, although the contraction-based clinical benchmark, i.e. ejection fraction, improves the classification performance significantly from the shape-based clinical benchmark, i.e. ES volume, the mesh classification network outperforms the clinical benchmark across all metrics and achieves a ∼6% increase in cross-validated AUROC scores.

Similar to our analysis of ES shapes, we also want to visualize 3D contraction patterns of cases that result in good and bad predictions by the network. To this end, we follow the same procedure as for the ES shape inputs to determine the network's prediction error for each case, and present in Fig. 4 the ED and ES 3D anatomies of patients that resulted in both good and bad predictions for both MACE and Non-MACE outcomes.

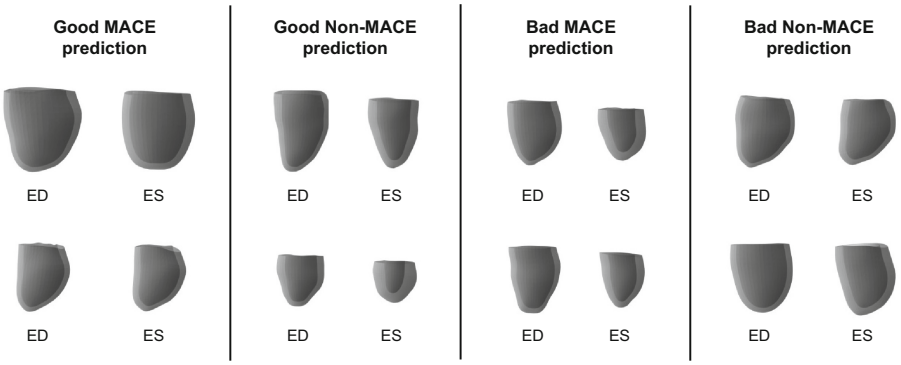

Fig. 4. Examples of input ED and ES meshes (in rows) that result in good (panels 1 and 2) and bad (panels 3 and 4) predictions of true MACE (panels 1 and 3) and Non-MACE (panels 2 and 4) cases by the contraction-based mesh classification network.

We observe that greater reductions in volumes and larger thickening of the myocardium between ED and ES phases lead to good predictions of Non-MACE outcomes. Similar to the ES shape results, bad predictions often occur when these associations between contraction and outcome are less present or reversed.

3.3 Effect of Class Imbalance

Since MACE outcomes are considerably less common than Non-MACE outcomes in our original dataset, we analyze next whether the patterns learned on the balanced dataset generalize well to more imbalanced datasets. To this end, we first create multiple datasets of both ES shapes and 3D contractions, each with larger levels of class imbalance between Non-MACE and MACE cases (2:1, 5:1, and 10:1). We achieve this by randomly sampling successively larger subsets from the remaining original dataset and then merging these subsets with the unseen test set of the balanced dataset used in the previous sections. We then apply the mesh classification networks and clinical benchmarks trained on the balanced dataset to each of the imbalanced datasets.

We find that while this results in a small decrease in AUROC scores for the ES shape-based mesh classification network compared to the balanced dataset, the scores for the 3D contraction-based mesh classification network and both clinical benchmarks show little change for higher levels of class imbalance. Finally, we repeat the same procedure for the full dataset (class imbalance of ∼13:1) and compare the results with both the clinical benchmarks and a previous machine learning-based approach [9] in Table 3.

We find that the mesh classification network achieves the highest AUROC scores for both ES shape and 3D contraction inputs with average improvements of ∼9% and ∼3% compared to the clinical and machine learning-based benchmarks, respectively.

Table 3. MACE prediction results on the original highly imbalanced dataset.

Input	Method	AUROC
ES volume	Regression	0.624
ES 3D shape	PCA + regression [9]	0.681
ES 3D shape	Mesh classification network	0.705
Ejection fraction	Regression	0.696
3D contraction	PCA + regression [9]	0.716
3D contraction	Mesh classification network	0.734

4 Discussion and Conclusion

In this work, we have presented a novel geometric deep learning approach to predict MACE outcomes from 3D cardiac anatomy and function data and found it capable of outperforming corresponding clinical benchmarks by considerable margins. On the one hand, this indicates that the full 3D shape representations of the heart, which enable the combined assessment of both global and local 3D shape features, contain more MACE-related information than the respective clinical metrics which are limited to a global cardiac function assessment with a single value. On the other hand, it demonstrates that the mesh classification network is adequately designed to successfully extract such multi-scale features for the purpose of MACE prediction. The outperformance of the respective clinical benchmarks by the pertinent networks was larger for ES shape inputs compared to 3D contraction inputs. We hypothesize that the considerably higher parameterization of the network compared to the regression model allows it to discover more intricate patterns in ES shapes, which implicitly provide relevant information about cardiac function and, in turn, help it achieve considerably improved prediction performance closer to the ones observed when modeling contraction explicitly.

The mesh-specific design of the network allows it to achieve these results by directly processing 3D surface mesh data in an efficient manner, and enables all network training to be conducted on a standard CPU. This is in contrast to voxelgrid-based deep learning approaches, which typically require high-powered GPU infrastructure for similar use cases.

In the visual analysis of the input heart shapes, we observe that small endocardial volume changes between ED and ES meshes typically lead to a correct MACE classification and vice versa for Non-MACE predictions. This is plausible from a clinical perspective as it is indicative of impaired cardiac contraction which in turn increases the risk of a future MACE outcome. Similarly, a large ES endocardial volume and small myocardial thickness at ES often cause the shape-based network to correctly classify cases as MACE. We hypothesize that such hearts can also implicitly be associated with poor contractive ability since both volume and thickness would typically be expected to have opposite characteristics at ES for healthy subjects. Both the shape- and contraction-based

networks make bad predictions when these associations that are present in the majority of cases are reversed. While this shows that the network has indeed learned useful patterns and applies them in a consistent and robust way, it also indicates that for some cases additional biomarkers apart from shape descriptors might be beneficial to further boost prediction performance.

We also find that the mesh networks trained on balanced datasets generalize well when applied to higher levels of class imbalance. This indicates that most of the 3D shape and contraction variability required for MACE classification are already present and extractable in the smaller balanced subset. The considerable outperformance over the clinical benchmark is also maintained by the mesh classification network in the original dataset with a large imbalance of about 13:1. This is particularly important for the applicability of the method in clinical practice where class imbalances between different outcomes are commonly encountered.

The mesh classification network also achieves higher AUROC scores for both ES shapes and contraction inputs of the fully imbalanced dataset than a machine learning-based approach, which combines principal component analysis with a binomial sigmoid regression model [9]. We attribute this finding to the higher number of trainable parameters and the presence of non-linearities in the deep learning network, giving it the ability to learn more complex feature relationships in the data. However, we note that this should only be interpreted as an approximate comparison, as the objective of the machine learning benchmark was not only to achieve the highest possible classification accuracy but also to retain high interpretability and clinical applicability. While our proposed deep learning approach comes with some potential comparative disadvantages, such as a more complex optimization process, longer training times, and possibly lower robustness, we find in our experiments that a careful design of the network architecture and training procedure tailored to the dataset at hand is sufficient to address these challenges and achieve the observed outperformance of both clinical and machine learning benchmarks. Hereby, the usage of a large mini-batch size and the introduction of dropout with an empirically determined probability of 0.3 are particularly important to regularize the network and improve training stability and generalizability to unseen test data. Furthermore, we believe that a larger number of MACE cases or the usage of data augmentation would likely further help the network to improve predictive performance and reach its full potential.

Acknowledgments. The authors express no conflict of interest. The work of MB is supported by the Stiftung der Deutschen Wirtschaft (Foundation of German Business). AB is a Royal Society University Research Fellow and is supported by the Royal Society (Grant No. URF\R1\221314). The work of AB and VG is supported by the British Heart Foundation (BHF) Project under Grant PG/20/21/35082. The work of VG is supported by the CompBioMed 2 Centre of Excellence in Computational Biomedicine (European Commission Horizon 2020 research and innovation programme, grant agreement No. 823712). The work of JCA is supported by the EU's Horizon 2020 research and innovation program under the Marie Sklodowska-Curie (g.a. 764738) and the EPSRC Impact Acceleration Account (D4D00010 DF48.01), funded by

UK Research and Innovation. ABO holds a BHF Intermediate Basic Science Research Fellowship (FS/17/22/32644). The work is also supported by the German Center for Cardiovascular Research, the British Heart Foundation (PG/16/75/32383), and the Wellcome Trust (209450/Z/17).

References

1. Beetz, M., Banerjee, A., Grau, V.: Biventricular surface reconstruction from cine MRI contours using point completion networks. In: 2021 IEEE 18th International Symposium on Biomedical Imaging (ISBI), pp. 105–109. IEEE (2021)
2. Beetz, M., Banerjee, A., Grau, V.: Generating subpopulation-specific biventricular anatomy models using conditional point cloud variational autoencoders. In: Puyol Antón, E., et al. (eds.) STACOM 2021. LNCS, vol. 13131, pp. 75–83. Springer, Cham (2022). https://doi.org/10.1007/978-3-030-93722-5_9
3. Beetz, M., Banerjee, A., Grau, V.: Multi-domain variational autoencoders for combined modeling of MRI-based biventricular anatomy and ECG-based cardiac electrophysiology. Front. Physiol., 991 (2022)
4. Beetz, M., Banerjee, A., Sang, Y., Grau, V.: Combined generation of electrocardiogram and cardiac anatomy models using multi-modal variational autoencoders. In: 2022 IEEE 19th International Symposium on Biomedical Imaging (ISBI), pp. 1–4 (2022)
5. Beetz, M., Ossenberg-Engels, J., Banerjee, A., Grau, V.: Predicting 3D cardiac deformations with point cloud autoencoders. In: Puyol Antón, E., et al. (eds.) STACOM 2021. LNCS, vol. 13131, pp. 219–228. Springer, Cham (2022). https://doi.org/10.1007/978-3-030-93722-5_24
6. Bello, G.A., et al.: Deep-learning cardiac motion analysis for human survival prediction. Nat. Mach. Intell. **1**(2), 95–104 (2019)
7. Chang, Y., Jung, C.: Automatic cardiac MRI segmentation and permutation-invariant pathology classification using deep neural networks and point clouds. Neurocomputing **418**, 270–279 (2020)
8. Corral Acero, J., et al.: The 'digital twin' to enable the vision of precision cardiology. Eur. Heart J. **41**(48), 4556–4564 (2020)
9. Corral Acero, J., et al.: Understanding and improving risk assessment after myocardial infarction using automated left ventricular shape analysis. JACC: Cardiovasc. Imaging (2022)
10. Corral Acero, J., et al.: Left ventricle quantification with cardiac MRI: deep learning meets statistical models of deformation. In: Pop, M., et al. (eds.) STACOM 2019. LNCS, vol. 12009, pp. 384–394. Springer, Cham (2020). https://doi.org/10.1007/978-3-030-39074-7_40
11. Corral Acero, J., et al.: SMOD - data augmentation based on statistical models of deformation to enhance segmentation in 2D cine cardiac MRI. In: Coudière, Y., Ozenne, V., Vigmond, E., Zemzemi, N. (eds.) FIMH 2019. LNCS, vol. 11504, pp. 361–369. Springer, Cham (2019). https://doi.org/10.1007/978-3-030-21949-9_39
12. Dalton, D., Lazarus, A., Rabbani, A., Gao, H., Husmeier, D.: Graph neural network emulation of cardiac mechanics. In: Proceedings of the 3rd International Conference on Statistics: Theory and Applications (ICSTA 2021), pp. 127-1-8 (2021)
13. Defferrard, M., Bresson, X., Vandergheynst, P.: Convolutional neural networks on graphs with fast localized spectral filtering. In: Proceedings of the 30th International Conference on Neural Information Processing Systems, pp. 3844–3852 (2016)

14. Di Folco, M., Moceri, P., Clarysse, P., Duchateau, N.: Characterizing interactions between cardiac shape and deformation by non-linear manifold learning. Med. Image Anal. **75**, 102278 (2022)
15. Eitel, I., et al.: Left ventricular global function index assessed by cardiovascular magnetic resonance for the prediction of cardiovascular events in ST-elevation myocardial infarction. J. Cardiovasc. Magn. Reson. **17**(1), 1–9 (2015)
16. Eitel, I., et al.: Intracoronary compared with intravenous bolus abciximab application during primary percutaneous coronary intervention in ST-segment elevation myocardial infarction: cardiac magnetic resonance substudy of the AIDA STEMI trial. J. Am. Coll. Cardiol. **61**(13), 1447–1454 (2013)
17. Fey, M., Lenssen, J.E.: Fast graph representation learning with PyTorch Geometric. In: ICLR Workshop on Representation Learning on Graphs and Manifolds (2019)
18. Ibanez, B., et al.: 2017 ESC guidelines for the management of acute myocardial infarction in patients presenting with ST-segment elevation: The task force for the management of acute myocardial infarction in patients presenting with ST-segment elevation of the european society of cardiology (ESC). Eur. Heart J. **39**(2), 119–177 (2018)
19. Kingma, D.P., Ba, J.: Adam: a method for stochastic optimization. arXiv preprint arXiv:1412.6980 (2014)
20. Lamata, P., et al.: An automatic service for the personalization of ventricular cardiac meshes. J. Roy. Soc. Interface **11**(91), 20131023 (2014)
21. Lu, P., Bai, W., Rueckert, D., Noble, J.A.: Modelling cardiac motion via spatio-temporal graph convolutional networks to boost the diagnosis of heart conditions. In: Puyol Anton, E., et al. (eds.) STACOM 2020. LNCS, vol. 12592, pp. 56–65. Springer, Cham (2021). https://doi.org/10.1007/978-3-030-68107-4_6
22. Lu, P., Bai, W., Rueckert, D., Noble, J.A.: Multiscale graph convolutional networks for cardiac motion analysis. In: Ennis, D.B., Perotti, L.E., Wang, V.Y. (eds.) FIMH 2021. LNCS, vol. 12738, pp. 264–272. Springer, Cham (2021). https://doi.org/10.1007/978-3-030-78710-3_26
23. Marcos-Garcés, V., et al.: Risk score for early risk prediction by cardiac magnetic resonance after acute myocardial infarction. Int. J. Cardiol. **349**, 150–154 (2022)
24. Meister, F., et al.: Graph convolutional regression of cardiac depolarization from sparse endocardial maps. In: Puyol Anton, E., et al. (eds.) STACOM 2020. LNCS, vol. 12592, pp. 23–34. Springer, Cham (2021). https://doi.org/10.1007/978-3-030-68107-4_3
25. Nestelberger, T., et al.: Predicting major adverse events in patients with acute myocardial infarction. J. Am. Coll. Cardiol. **74**(7), 842–854 (2019)
26. Paszke, A., et al.: PyTorch: an imperative style, high-performance deep learning library. In: Proceedings of the 33rd International Conference on Neural Information Processing Systems, pp. 8026–8037 (2019)
27. Ranjan, A., Bolkart, T., Sanyal, S., Black, M.J.: Generating 3D faces using convolutional mesh autoencoders. In: Proceedings of the European Conference on Computer Vision (ECCV), pp. 704–720 (2018)
28. Reindl, M., Eitel, I., Reinstadler, S.J.: Role of cardiac magnetic resonance to improve risk prediction following acute ST-elevation myocardial infarction. J. Clin. Med. **9**(4), 1041 (2020)
29. Suinesiaputra, A., et al.: Statistical shape modeling of the left ventricle: myocardial infarct classification challenge. IEEE J. Biomed. Health Inf. **22**(2), 503–515 (2017)
30. Thiele, H., et al.: Effect of aspiration thrombectomy on microvascular obstruction in NSTEMI patients: the TATORT-NSTEMI trial. J. Am. Coll. Cardiol. **64**(11), 1117–1124 (2014)